ADVANCES IN ATMOSPHERIC SCIENCES, VOL. 23, NO. 5, 2006, 815–830

Application of ATOVS Microwave Radiance Assimilation to Rainfall Prediction in Summer 2004

QI Linlin*[1,3] (齐琳琳) and SUN Jianhua[2] (孙建华)

[1] *Chinese Academy of Meteorological Sciences, Beijing* 100081

[2] *Laboratory of Cloud Physics and Severe Storms, Institute of Atmospheric Physics, Chinese Academy of Sciences, Beijing* 100029

[3] *Institute of Aviation Meteorology, Beijing* 100085

(Received 3 November 2005; revised 17 May 2006)

ABSTRACT

Experiments are performed in this paper to understand the influence of satellite radiance data on the initial field of a numerical prediction system and rainfall prediction. First, Advanced Microwave Sounder Unit A (AMSU-A) and Unit B (AMSU-B) radiance data are directly used by three-dimensional variational data assimilation to improve the background field of the numerical model. Then, the detailed effect of the radiance data on the background field is analyzed. Secondly, the background field, which is formed by application of Advanced Television and Infrared Observation Satellite Operational Vertical Sounder (ATOVS) microwave radiance assimilation, is employed to simulate some heavy rainfall cases. The experiment results show that the assimilation of AMSU-A (B) microwave radiance data has a certain impact on the geopotential height, temperature, relative humidity and flow fields. And the impacts on the background field are mostly similar in the different months in summer. The heavy rainfall experiments reveal that the application of AMSU-A (B) microwave radiance data can improve the rainfall prediction significantly. In particular, the AMSU-A radiance data can significantly enhance the prediction of rainfall above 10 mm within 48 h, and the AMSU-B radiance data can improve the prediction of rainfall above 50 mm within 24 h. The present study confirms that the direct assimilation of satellite radiance data is an effective way to improve the prediction of heavy rainfall in the summer in China.

Key words: heavy rainfall, satellite radiance data, direct assimilation, rainfall prediction experiments

doi: 10.1007/s00376-006-0815-6

1. Introduction

With the development of numerical models during the past several decades, they can give objective, quantitative, and standard weather predictions. However, the quality of the quantitative prediction of heavy rainfall is still very low up to the present. Many previous studies have indicated that the dynamical and physical schemes are mature in numerical models, therefore, the improvement of heavy rainfall prediction should now depend more on the initial field. It is well known that accurate initial conditions are very important in the simulation of heavy rainfall. For a long time, routine soundings were made only twice per day, and moreover, these were not made over the sea to the east of China or over western China, so the lack of sufficient observational data has been one of the major obstacles in predicting the heavy rainfall accurately in China. With the development of numerical models and progress in atmospheric remote sensing techniques, meteorological satellites can cover a large area and obtain higher spatial resolution atmospheric information, therefore, the use of satellite data in numerical models could solve the problem of sparse conventional data in the depopulated zones of the ocean, plateau, and desert.

With the advancement in remote sensing and data analysis techniques, it is now possible to use satellite radiance data for improving the initial analysis and the precipitation prediction in general. Much research has made use of satellite data in the models for improving the prediction. For instance, Smith et al. (1985) and Menzel and Chedin (1990) pointed out that the vertical profiles of temperature and humidity retrieved

*E-mail: niceqll@mail.iap.ac.cn

from satellite observations have played important roles both in the analysis of current weather conditions and in the prediction of the future status of the atmosphere. Wolcott and Warner (1981) and Jiang et al. (1994) applied satellite data and rainfall observation for modifying the initial humidity field in a numerical simulation. Ninomiya and Kurihara (1987) made use of IR satellite data for the forecast of a long-lived mesoscale convective system in the Baiu frontal zone. Turpeinen et al. (1990) incorporated the latent heat forcing from IR and VIS satellite data into the Canadian Regional Finite-Element Model with static initialization. Ge et al. (1998, 2000) applied both radar and satellite data for the real-time numerical prediction of heavy rainfall and obtained better results. Recently, the weather research prediction program in the United States also focused on the high-resolution data from satellite and radar to improve the quantitative prediction of rainfall. It is widely established that assimilating satellite data helps to improve the quality of weather forecasts, and soundings retrieved from microwave remote sensing have been proven to be the most informative sources of data to provide significant improvements in the quantitative measurements of atmospheric variables.

Based on the advantages of satellite radiance data, we study the impact of their application on the initial field of the model and the rainfall intensity prediction in summer. In this paper, five parts will be presented. The introduction is given in section 1. In section 2, the characteristics of satellite radiance data and their application methods are briefly introduced. The analyses of the assimilation results of satellite radiance data and the rainfall prediction experiments are carried out in sections 3 and 4, respectively. Finally, a summary and conclusions are given in section 5.

2. Satellite radiance data and their application

The second satellite of the advanced NOAA (National Oceanic and Atmospheric Administration) polar orbiting satellite series, NOAA-16, was launched in 2000 and the operational distribution of data started in April 2001. The new system is composed of two sun-synchronous polar orbiting spacecraft, one of which is in a morning orbit (AM) and the second is in an afternoon (PM) orbit. NOAA-15 and NOAA-16 are for the morning and afternoon orbits, respectively. Recently, NOAA-17 was launched to replace NOAA-15. Therefore, NOAA-16 and NOAA-17 are the fifth generation polar-orbiting routine environmental series satellites. The Advanced Microwave Sounding Unit (AMSU) on NOAA-16 and NOAA-17 consists of type A (AMSU-A) with 15 channels and type B (AMSU-B) with 5 channels, which are used to improve the vertical sounding of the atmospheric temperature and humidity and to monitor the surface parameters. In addition, the high-resolution microwave sounding unit AMSU-B can be used to improve the sounding of the atmospheric humidity. In comparison with the conventional infrared and visible light sounding units, the AMSU units have the unique ability to penetrate heavy clouds to sound the vertical structure of the atmospheric temperature and humidity (Weng and Grody, 2000).

AMSU radiance brightness temperature data are obtained from the L1d dataset of the National Satellite Meteorological Center (NSMC). This dataset is generated by using the Advanced TIROS Operational Vertical Sounder (ATOVS) preprocessing software package after decoding, calculating the orientation, scaling, and brightness temperature, and correcting the brightness temperature and mutually matching the data of many instruments (Zhang, 2002).

In 2004, the AMSU-A radiance brightness temperature data of NOAA-17 experienced some trouble, so the AMSU-A and AMSU-B microwave radiance data of NOAA-16 and the AMSU-B microwave radiance data of NOAA-17 are used in the present study.

2.1 *The application methods of satellite radiance data*

The difficulty of satellite radiance data application in the model is that the meteorological satellite observes heat radiances and cannot detect the atmospheric variables of temperature and moisture directly. There exists a complicated nonlinear relationship between thermal radiances and atmospheric variables, so the conventional spatial interpolation method cannot be used. In numerical weather prediction, there are two main methods to apply satellite radiance data. First, satellite sounding radiance data are retrieved to compute the atmospheric variables of temperature and humidity by using the physical retrieval method, and then the retrieved data are assimilated as conventional observation data (Zhu et al., 2000). In practice, this method has the ill-posedness problem in the retrieval calculation, so the application of satellite radiance data by this method has little or a negative effect on the rainfall forecast (William, 1991). To overcome the above-mentioned difficulty, the direct variational assimilation of the satellite data was adopted as the second method (Courtier et al., 1996, Courtier, 1997, Lorenc, 1997). The fundamental idea is that the simulated radiance are calculated by using atmospheric variables through the radiance transfer equation. And then the differences between the simulated radiance

and the observed radiance are obtained by the data assimilation system. Under certain constraint conditions, in constructing a cost function, and by using an optimal method, the analysis variables closest to the real atmosphere are obtained in the minimization process (Eyre et al., 1993, Andersson et al., 1994, Rabier et al., 2000).

As is well-known, the radiance data used directly by the variational assimilation method can avoid the error caused by the computation of the complex ill-posed problem in the retrieval computationally. The variational assimilation method not only analyzes the satellite radiance data with the complex nonlinear function of the model variables and integrates the retrieval and the analysis in one step, but it also effectively combines the observational data from different sources of different kinds and with different error characteristics together. At present, several operational centers, such as the ECMWF (European Center for Medium-Range Weather Forecasts) and NCEP (National Centers for Environmental Prediction), make use of the routine 3D/4D variational assimilation systems. Some experiments have showed that the microwave radiance data from the Television and Infrared Observation Satellite Operational Vertical Sounder (TOVS) on the NOAA polar-orbiting satellites, especially the AMSU, may apparently reduce the errors of the numerical weather prediction. The method, using the 3D/4D variational technique to assimilate the satellite observations directly, might obtain a more accurate description of the atmospheric state and the valid prediction can be extended by 1/4 day. (Courtier et al., 1996; Derber and Wu, 1998; McNally et al., 1999).

Recently, several studies have been carried out in China on the applications of satellite radiance data in numerical prediction. A preliminary contrast study, using HIRS/2 (High Resolution Infrared Sounder) radiance data and conventional radiosonde data, showed that the results of direct assimilation of radiance data are better than that of the retrieval product (Wang et al., 1995). Another study showed that initial fields on the Tibetan Plateau could apparently be improved with the use of TOVS radiance data in the MM5 model (Weng and Xu, 1999). Qi (2003) used ATOVS radiance data, conventional radiosonde data and NCEP reanalysis data to form the initial field of MM5 and simulated the heavy rainfall in Shanghai on 5–6 August 2001. The results showed that the location and intensity of the simulated heavy rainfall using the ATOVS radiance data are better than that of only using conventional observed data. Pan et al. (2003) performed comparison experiments with and without AMSU-A data for simulating a very heavy rainstorm that occurred in the Wuhan City area during 21–22 July 1998. The simulation results showed that the forecasts of temperature and the mixing ratio of water vapor were better in experiment with AMSU-A data than in that without AMSU-A data. But the precipitation forecasts of experiments with AMSU-A do not seem superior to that without AMSU-A. Zhang et al. (2004) used ATOVS microwave radiance data to simulate the track of typhoon Rammasun. The study showed that the direct assimilation of ATOVS microwave radiance data can improve the typhoon track prediction. Although many studies have been done by Chinese meteorologists, most of the above-mentioned works only focus on case studies, which cannot give statistical results of the detailed influences of satellite radiance data on the rainfall prediction over China. Therefore, based on the studies mentioned above, we further study the impact of AMSU-A and AMSU-B radiance data on the initial field of a numerical model and the rainfall prediction.

2.2 *A general description of GRAPES_3D-VAR system*

In this study, the three-dimensional variational data assimilation (3D-VAR) system of the Global/Regional Assimilation PrEdiction System (GRAPES) developed by the Chinese Meteorology Administration (CMA) was used as the tool to assimilate the radiance data. In 2001, CMA launched a national key project to develop the next generation of the Numerical Weather Prediction (NWP) system GRAPES. The data assimilation system is one of the key factors in a numerical prediction system for research as well as for operation, so the GRAPES_3D-VAR system was first developed in this project. The basic goal of the 3D-VAR system is to produce an "optimal" estimate of the true atmospheric state at analysis time through the iterative solution of a defined cost function. In general, a cost function for 3D-VAR is defined as the following equation:

$$
\begin{aligned}
J &= J_{\mathrm{b}} + J_{\mathrm{o}} \\
J_{\mathrm{b}} &= \frac{1}{2}(x_{\mathrm{b}} - x)^{\mathrm{T}} \boldsymbol{B}^{-1}(x_{\mathrm{b}} - x) \\
J_{\mathrm{o}} &= \frac{1}{2}[H(x) - y_{\mathrm{o}}]^{\mathrm{T}} \boldsymbol{O}^{-1}[H(x) - y_{\mathrm{o}}] \qquad (1)
\end{aligned}
$$

where x is the model state; x_{b} is the background state; $\boldsymbol{B}$ is the background error covariance matrix; $\boldsymbol{O}$ is the observation error covariance matrix; J_{b} and J_{o} are the cost function of background and observation respectively; the operator H is the mapping operator with some complex structure transform from the model space to the observation space; and y_0 is the

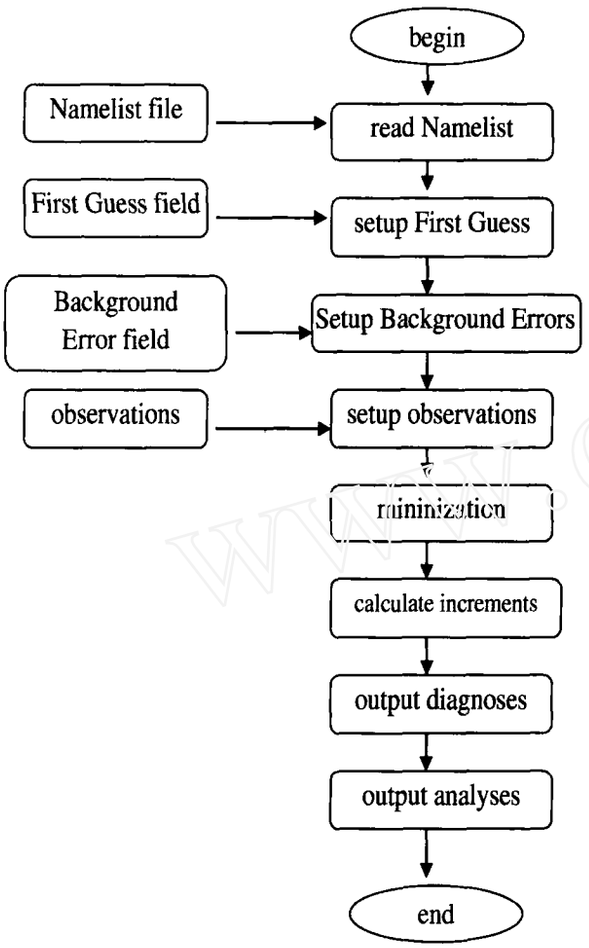

Fig. 1. The 3D-VAR assimilation system flow chart.

observation operator which converts the model state to the observation state.

In GRAPES_3D-VAR, the quasi-Newton minimization technique is used to obtain the minimum of the cost function. The background error covariance matrix is a statistic based on the model variables. We adopt the "NMC" method (Parrish and Derber, 1992), used by the U. S. National Meteorological Center, to construct mono-variant covariance matrixes for each three-dimensional field. For a certain model variable, the background errors are computed at all the vertical levels of every horizontal grid point. The main features and flow chart (Fig. 1) of GRAPES_ 3D-VAR are as follows: (1) The analysis is the incremental in the model varaible and conducted on the mandatory level; (2) A latitude-longitude horizontal grid is specified for a limited area; (3) A non-staggered Arakawa-A grid scheme is used for the horizontal grid distribution; (4) The observation operators are available to assimilate both the conventional data and unconventional datasets (such as ATOVS radiance, etc.); (5) The model variables are geopotential height or temperature, horizontal wind components, specific humidity or relative humidity. The analysis variables are defined as the stream function, unbalanced potential velocity, unbalanced height or temperature, relative humidity or specific humidity; (6) A simple geostrophic relationship (or a linear balance equation) is employed for the mass/wind balance; (7) The recursive filter is approximately used for the horizontal correlations, and the EOFs are used for the vertical correlations (Xue et al., 2001).

2.3 *Quality control of ATOVS radiance data in the GRAPES_3D-VAR system*

Many reasons can cause big errors in the satellite observations, such as the weather conditions (clear, cloudy and overcast), the surface conditions (sea surface, land, sea ice, etc.), and the accuracy of the sensor, therefore quality control is necessary in the assimilation analysis, including checks for extreme values, a deviation check between the estimated values from the background fields and the observation data, the cloud detection, and channel selection.

(1) Extreme value check. The radiance brightness temperature within the range 150–350°C are used, and the others are rejected.

(2) The deviation check between the estimated values and the observation data. A threshold check is only used. The radiance brightness temperature data that do not satisfy the following inequality

$$|y_{\mathrm{b}i} - y_{\mathrm{o}i}| \leqslant k\sigma \tag{2}$$

are excluded, where $y_{\mathrm{b}i}$ and $y_{\mathrm{o}i}$ are the background fields of the simulated observation and the actual observation in channel i, respectively; σ is the covariance of radiance brightness temperature data; k is the factor.

(3) The cloud detection. Although the AMSU has the ability to penetrate the cloud layer to detect the atmospheric temperature and humidity, the scattering by water drops and ice crystals in the precipitation cloud, which are larger than the radiance wavelength, can weaken the signal below the cloud layer. It influences the detection, thus the precipitation cloud must be checked. According to the precipitation probability (%) of the ATOVS dataset, we use

$$P = [1 + e^{-(10.5+0.184T_{\mathrm{B1}}-0.221T_{\mathrm{B15}})}]^{-1} \tag{3}$$

Where, T_{B1} and T_{B15} are the observation brightness temperatures in channel 1 and channel 15, respectively. When $P \geqslant 70$, the radiance brightness temperature must be rejected.

(4) Channel selection. The channel selection is decided according to the peak energy contribution level

of the sounder channel and the influence of the sounding objective on the retrieval results of temperature and water vapor. In order to avoid the negative influence of the surface albedo on the retrieval results of temperature and water vapor, channels 1–4 of the microwave sounder AMSU-A and channels 1–2 of AMSU-B are excluded. Channels 12–15 of the microwave sounder AMUS-A are also excluded to avoid the error caused by the interpolation above the model top level which might influence the retrieval results of temperature and water vapor.

3. Analysis on direct assimilation of ATOVS radiance data

3.1 *The experiment designs*

In order to understand the ability of the GRAPES_3D-VAR with ATOVS radiance data, three regional experiments were carried out. In the three experiments, the AMSU-A, AMSU-B and AMSU (AMSU-A+AMSU-B) radiance data of the polar-orbiting satellites NOAA-16 and NOAA-17 from May to August 2004 were used for analysis, respectively. The background fields are the $1° \times 1°$ NCEP reanalysis data in each experiment, including the geopotential height, the temperature, the horizontal wind velocity and the relative humidity. The analysis domain was 0°–70°N, 60°–160°E with a resolution of $1.0° \times 1.0°$ in the horizontal and 17 layers in the vertical. The cost function, the background error and observation error matrix were all defined as default in the CMA's GRAPES_3D-VAR system. The time window of GRAPES_3D-VAR is set as three hours, so the analysis results can be obtained at 0000 UTC, 0600 UTC, 1200 UTC, and 1800 UTC for every day as the radiance data become available.

In the following, the analysis results of the GRAPES_3D-VAR with ATOVS data are shown by the RMSE (Root Mean Squared Error), which is often used to evaluate the accuracy between the analysis results and observations. The RMSE, calculated by the results of each experiment, can indicate whether the satellite radiance data have an impact on the background or not.

The formula of the RMSE is:

$$\mathrm{RMSE} = \left[\frac{1}{N}\sum_{i=1}^{N}(A_{\mathrm{s}i} - A_{\mathrm{b}i})^2\right]^{\frac{1}{2}} \tag{4}$$

Where A_{si} and A_{bi} are values of the experiment results and background at grid i, respectively.

Usually, a large RMSE indicates that the satellite radiance assimilation has an obvious impact on the background field of the model. In the following part of the present section, the RMSE values of the monthly averaged geopotential height, temperature, relative humidity and horizontal wind at 1800 UTC at 1000, 925, 850, 700, 600, 500, 400, 300, and 250 hPa were analyzed.

3.2 *The impact on the temperature of the background field*

As we know, the AMSU-A radiance data mainly detect the temperature, but the AMSU-B radiance data mainly detect the humidity below 400 hPa. Due to the limitations of the type, quantity and resolution of the satellite data and background data, we will try to give some reasonable explanation for the statistical results of the assimilation experiments.

Figure 2 gives the monthly averaged RMSE of the temperature in experiments AMSU-A, AMSU-B and AMSU from May to August 2004. The analysis results show that the assimilations of AMSU-A, AMSU-B or AMSU almost have the same impact on the temperature of the background below 600 hPa and they have different impacts at the middle and upper levels. It is also found that the RMSE of the temperature decreases from 1000 hPa to 600 hPa in the three experiments. The RMSE of the temperature changes little from 600 hPa to 250 hPa in the AMSU-A experiment and from 600 hPa to 400 hPa in the AMSU-B experiment, but it increases remarkably at the upper level in the AMSU-B experiment.

From the above analyses, it is revealed that the impacts of the AMSU-A and AMSU-B radiance data on the temperature of the background field are obvious and almost the same at the lower level. Moreover, the RMSE values of the three experiments also show that the impact of radiance data on the temperature of the background field is less at the middle and upper levels than that at the lower level. According to the fact that the impact of the AMSU-A and AMSU-B radiance data on the background temperature is less between the peak energy contribution levels, we deduce that the different impacts on the background temperature at different levels may be related to the vertical distribution of peak energy of the microwave sounders AMSU-A and AMSU-B. In addition, it is well-known that most of the relatively smaller systems exist in the lower troposphere, and the routine observations cannot obtain information about them because of their lower horizontal resolution, but satellite data can discover the mesoscale/microscale systems because of their higher horizontal resolution, which may be why the radiance data impact the lower troposphere significantly. Furthermore, although the AMSU-B radiance data mainly detect the humidity, the temperature can be affected through the thermodynamic dynamical constraint relation in the variational assimilation system.

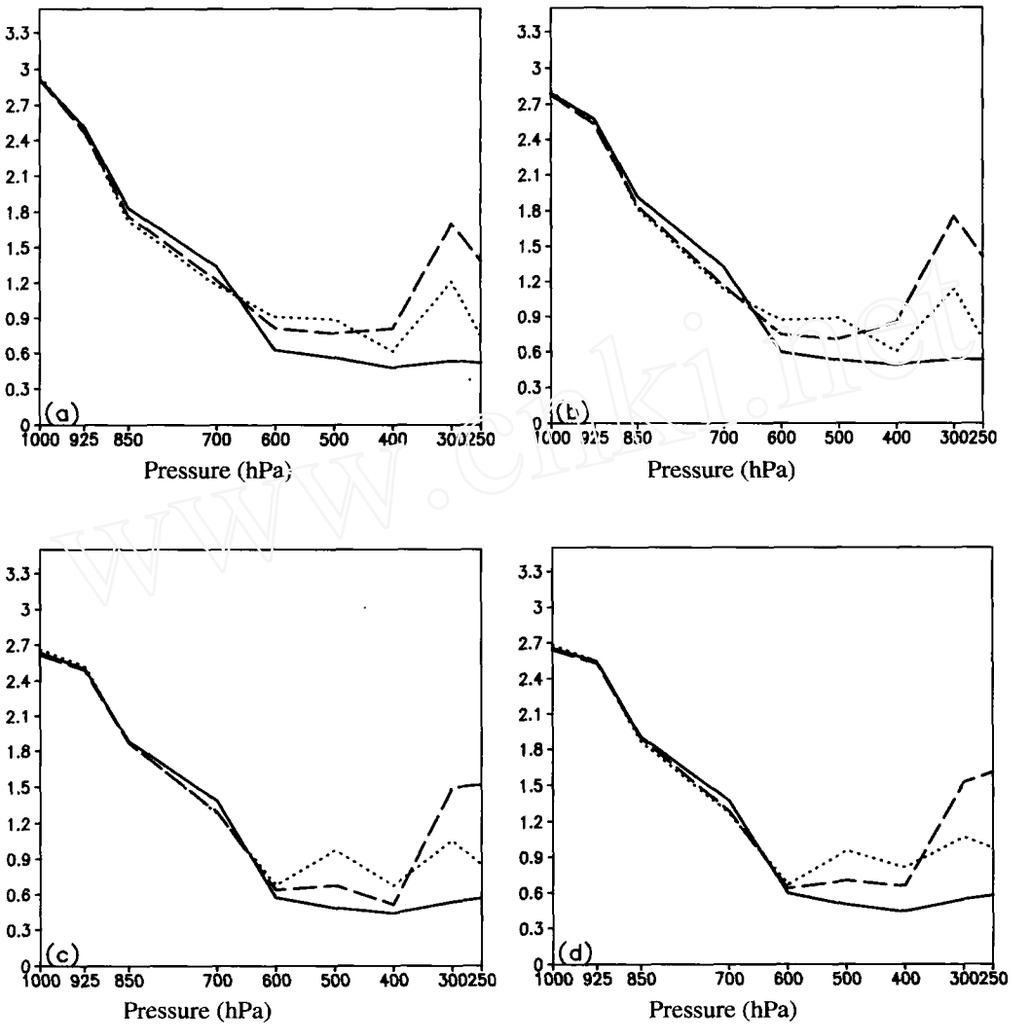

Fig. 2. The monthly averaged RMSE of the temperature in the AMSU-A, AMSU-B and AMSU experiments at 1800 UTC from May to August 2004: (a) May, (b) June, (c) July, (d) August (solid line: AMSU-A; long dashed line: AMSU-B; dotted line: AMSU).

3.3 *The impact on the relative humidity of the background field*

Figure 3 gives the monthly averaged RMSE of the relative humidity in the AMSU-A, AMSU-B and AMSU experiments from May to August 2004. The RMSE of the relative humidity decreases from 1000 hPa to 600 hPa in the three experiments and changes little from 600 hPa to 250 hPa in the AMSU-A experiment. The RMSE of the relative humidity also does not change too much from 600 hPa to 400 hPa, but it increases at the upper level remarkably in the AMSU-B experiment.

By analyzing the results of the three experiments, it is found that the influence of the AMSU-A data on the relative humidity is more obvious in the lower troposphere than in the middle and upper troposphere, while the influence of the AMSU-B data on the relative humidity is more significant in the whole troposphere. As we know, the humidity is an important factor for the prediction of the mesoscale/microscale systems, therefore, the assimilation of the AMSU-B data is also very important in the initial field. It is found that the impacts on the relative humidity in the AMSU-B and AMSU experiments are consistent and obviously increase near 300 hPa, which imply that assimilation of the AMSU-B data has a larger impact on the relative humidity of the background field at the upper level than that in the AMSU-A experiment. The obvious impact on the relative humidity above 300 hPa in the AMSU-B experiment may be related with the vapor absorption of the microwave radiation in the

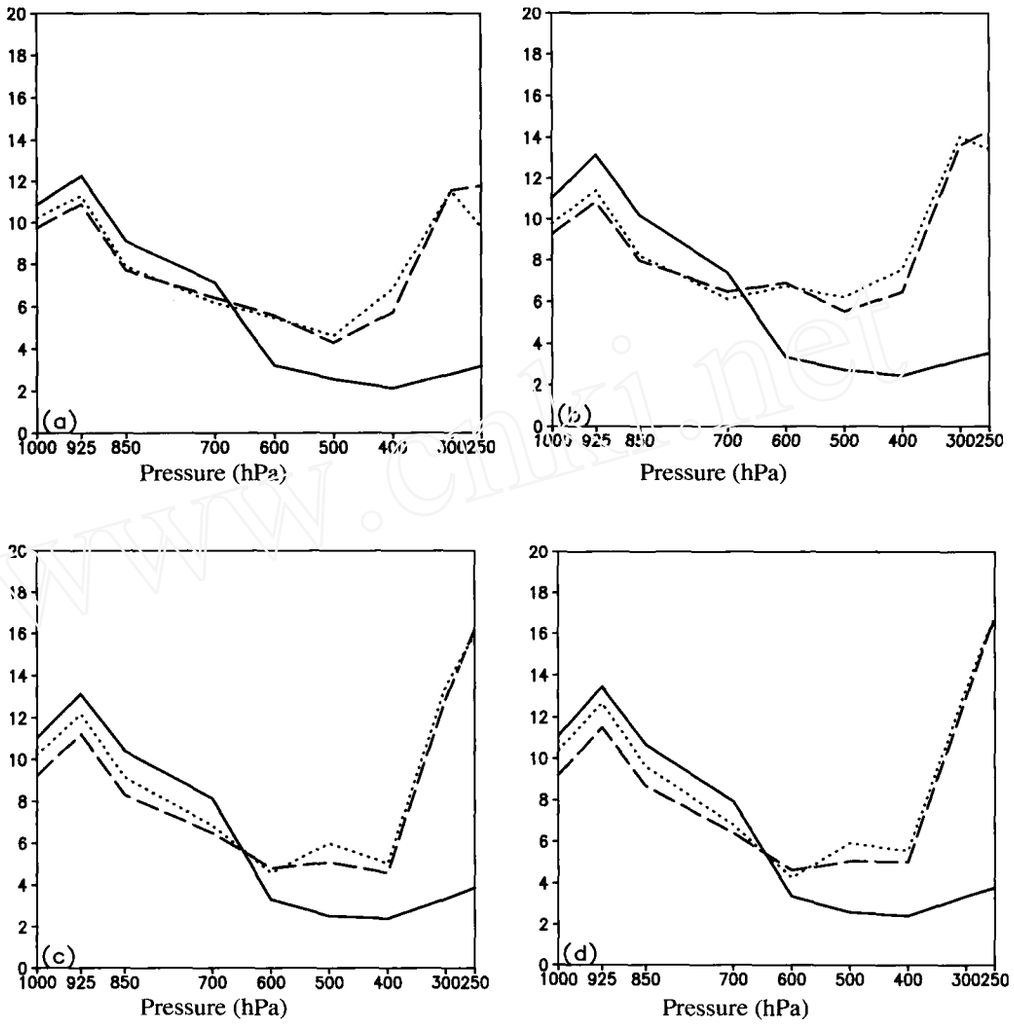

Fig. 3. The same as Fig. 2, but for the relative humidity.

upper troposphere in the fast radiative transfer model RTTOV (Radiative Transfer for TIROS Operational Vertical Sounder), which is adopted as the observation operator of the satellite radiance data in the GRAPES_3D-VAR. In its processing, the microwave radiation is absorbed by the vapor in the upper troposphere (above 300 hPa). In a word, the impacts on relative humidity in the AMUS-B experiment are more important in the upper troposphere.

3.4 *The impacts on the geopotential height and horizontal wind of the background field*

Figure 4 shows the monthly averaged RMSE of the geopotential height in the AMSU-A, AMSU-B and AMSU experiments from May to August 2004. The analysis results show that the assimilations of the AMSU-A and AMSU-B radiance data both have a certain impact on the geopotential height of the background. The RMSE values of the AMSU-A and AMSU-B experiment are almost the same in the lower level and increase from the middle level to the upper level. Nevertheless, the RMSE of the AMSU-B experiment has a significant variation near 300 hPa. The impact of the AMSU-A radiance data on the geopotential height of the background field is a little greater than that of the AMSU-B at the low-level, while the impact of the AMSU-B experiment is the most remarkable at the middle and upper level. Besides this, the RMSE values of the three experiments also show that the impact of the satellite radiance data on the geopotential height of the background field at the low troposphere is less than that at the middle and upper troposphere.

In addition, the monthly averaged RMSE values of horizontal wind in the AMSU-A, AMSU-B and AMSU

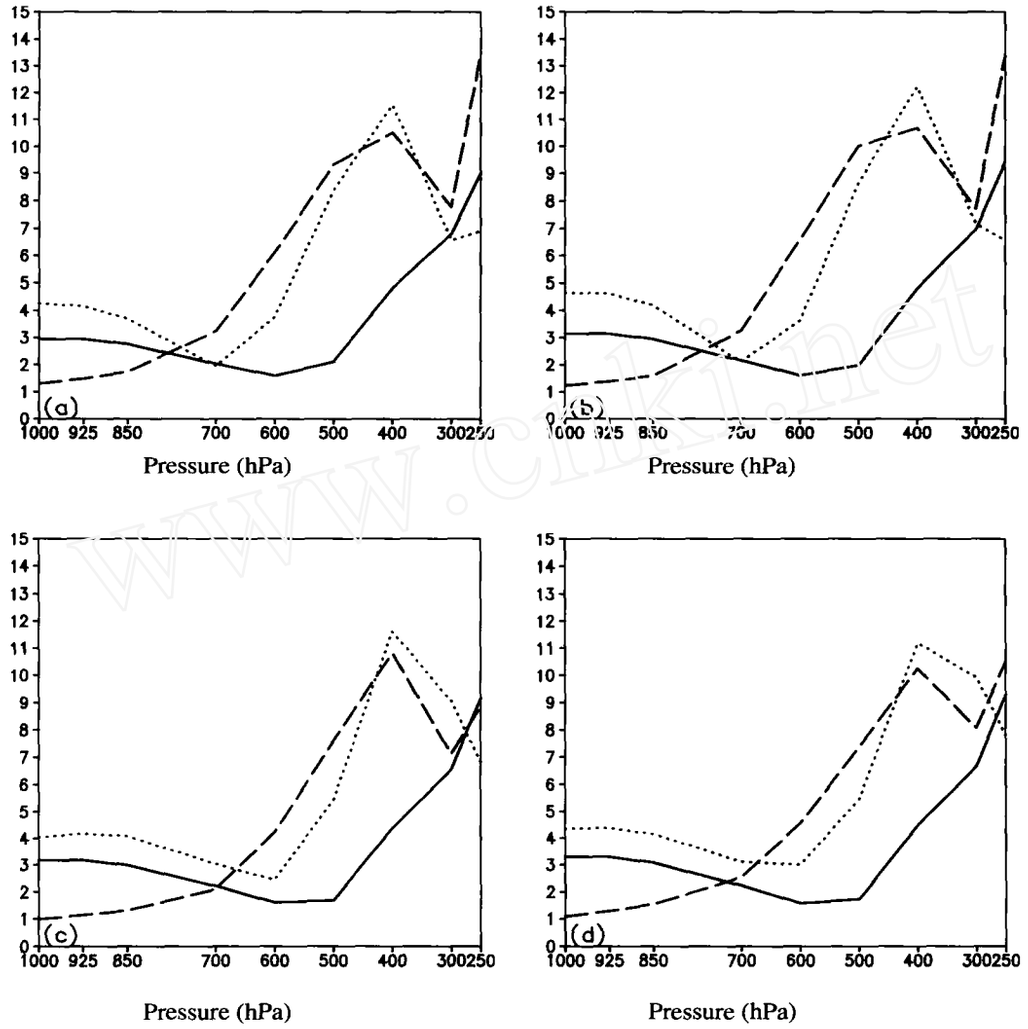

Fig. 4. The same as Fig. 2, but for the geopotential height.

experiments from May to August 2004 show that the impacts of satellite radiance data on horizontal wind are very similar to that of geopotential height.

With regard to the impacts on the geopotential height and wind field, it may be explained that despite the fact that the satellite data cannot directly offer information on the geopotential height and wind field, through the dynamical constraint relation in the variational assimilation process, the geopotential height and wind field can be modified valuably.

We have discussed the influences of the AMSU-A and AMSU-B radiance data on the temperature, relative humidity, geopotential height and wind field, and it was revealed that assimilation of satellite radiance data impacts the background field significantly. The temperature is modified obviously in the lower troposphere, and the geopotential height and flow field are obviously affected at the middle and upper troposphere. Nevertheless, the impacts on relative humidity are evident not only in the lower troposphere, but also in the upper troposphere. But the 3D-VAR system is very complicated, and many factors could influence the analysis results, such as the observation error, the interpolation of the background grid data onto the grid of observed brightness temperature data, and an extrapolation above the top level and below its bottom level. So the impacts of the satellite data on the background field are very complicated and it cannot be confirmed which is better at present.

Besides the above, the analysis results show that the impacts of satellite radiance data on the temperature, relative humidity, geopotential height and wind field of the background field are mostly similar in the different months in the summer of 2004.

4. Numerical experiments of rainfall

According to the above analysis, the impact of AMSU radiance data on the initial fields of the numerical simulation is obvious. Now we will do some numerical rainfall experiments and pay attention to the impact of initial field on the simulation results of precipitation, temperature and humidity.

4.1 *The configurations of the experiment*

The PSU-NCAR nonhydrostatic mesoscale model MM5V3 (Dudhia, 1993, Grell et al., 1994) is employed as the experimental numerical model. The cases, including the rainfalls occurring in the Yangtze River basin from 13 to 28 June 2004 and in North China on 10, 11, 16, 18 July and 3, 9, 10, 11, 13, 15, 24 August 2004, are adopted as experimental examples. In this paper, the goal is to examine the statistical results of AMSU-A and AMSU-B radiance data on the rainfall prediction. So we do not use all of the radiance data together. In order to understand the influence of different initial fields, the three experiments named CONT, COMPARE1 and COMPARE2 are carried out (Table 1).

In all experiments, besides the initial field being formed in a different way, the other schemes are the same. A two-way interactive, nested grid system including two domains is used (not shown). It consists of a 45-km grid domain (D01, 120×100 grid points) and a 15-km grid domain (D02, 163×142 grid points), which only covers China and is smaller than the domain of the GRAPES_3D-VAR analysis experiments in section 3. There are 30 vertical layers. The mixed-phase microphysics scheme is used, in which five prognostic equations are solved for the mixing ratios of water vapor, cloud water, rainwater, cloud ice, and snow. The Grell cumulus parameterization scheme is employed for subgrid-scale convection. The Blackadar high-resolution scheme is adopted to calculate the turbulent fluxes in the planetary boundary layer (PBL), while the relaxation boundary conditions are used in the lateral boundary. The cloud radiation scheme is used for processes of the atmospheric longwave and shortwave radiance parameterizations. In each experiment, the D01 and D02 both start at 0000 UTC and give a 48-h forecast.

Only the NCEP reanalysis data are used in the CONT experiment. In the COMPARE1 and COMPARE2 experiments, the assimilation results of the AMSU-A experiment and AMSU-B experiment, respectively, in section 3 are adopted to form the initial fields of both D01 and D02. In the following part, we analyze the simulated temperature and humidity field first, and then we analyze the rainfall prediction.

4.2 *Analysis of the experimental results of the temperature and humidity*

Figure 5 gives the averaged RMSE of the 24-h simulated temperature in CONT, COMPARE1 and COMPARE2. It is found that the RMSE of the simulated temperature is the same from 925 hPa to 100 hPa in the three experiments. The RMSE in COMPARE2 is the least while the RMSE in COMPARE1 is larger than that in CONT above 700 hPa. It is revealed that the impact of the AMSU-A and AMSU-B radiance data on the simulated temperature is obvious. Moreover, the RMSE values of the three experiments also show that the influence of the radiance data on the simulated temperature is less in the middle troposphere than in the lower and upper troposphere. The above analyses are consistent with the findings on impact of satellite radiance data on the background temperature in section 3. It is further confirmed that the simulated temperature can be affected through the thermodynamic dynamical constraint relation, even though the AMSU-B radiance data mainly detect the humidity.

Figure 6 gives the averaged RMSE of the 24-h simulated relative humidity in CONT, COMPARE1 and COMPARE2. The results show that the RMSE of relative humidity is larger than that of temperature in the troposphere. The RMSE of the relative humidity in COMPARE2 is mostly the same from 1000 hPa to 700 hPa, and it increases above 700 hPa. In total, the RMSE in COMPARE2 is the least while the RMSE in COMPARE1 is the largest in the whole troposphere.

In a word, the simulated results in the lower and middle levels are better than that in the upper level in the three experiments, and the results of COMPARE2 are the best.

Table 1. Experiment Schemes.

Experiment	Initial Scheme
CONT	Only the NCEP reanalysis data
COMPARE1	NCEP+AMSU-A analysis result from AMSU-A experiment in section 3
COMPARE2	NCEP+AMSU-B analysis result from AMSU-B experiment in section 3

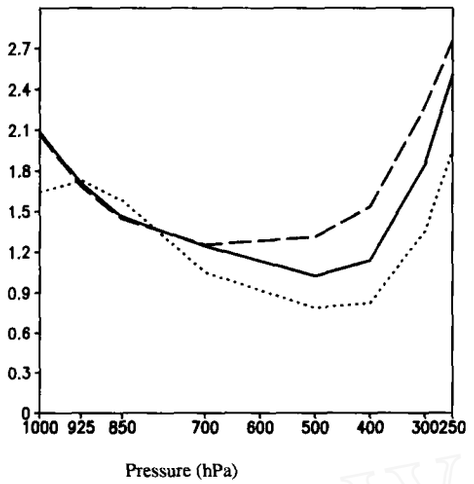

Fig. 5. The averaged RMSE of the 24-h simulated temperature for all cases in CONT, COMPARE1 and COMPARE2 (solid line: CONT; long dashed line: COMPARE1; dotted line: COMPARE2).

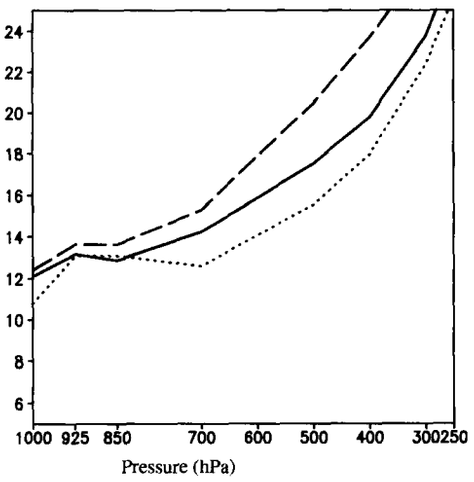

Fig. 6. The same as Fig. 5, but for the relative humidity.

4.3 *Analysis of the experimental results of the rainfall*

On the basis of the simulated temperature and relatively humidity analyses, in order to understand the impact of the initial field formed by the satellite radiance data on the rainfall prediction, the T_s score of 1 mm, 5 mm, 10 mm, 25 mm, 50 mm are calculated over the Region 1 (33°–50°N, 105°–125°E, North China) and Region 2 (20°–50°N, 95°–125°E, including South China, the Yangtze River Basin and North China) from the three experiments (Table 2). The T_s scores of the three experiments indicate that the prediction of heavy rainfall above 50 mm within 24 h improved significantly in the COMPARE2 experiment. And rainfall prediction above 10 mm improved in the COMPARE1 experiment. In comparison with the results of the CONT experiment, the T_s scores of 10, 25, and 50 mm improve 2%, 1.9%, and 2.6% within 24 h in Region 2 in the COMPARE1 experiment. The changes mentioned above in Region 1 are 2.1%, 3.2%, and 13%, and they are greater than those of Region 2. The rainfall prediction of 24–48 h indicates that using the initial field formed by the AMSU-A radiance data could distinctly improve the 10 and 25 mm rainfall prediction. The T_s scores of 10, 25, and 50 mm in 24–48 h forecast improved 0.4%, 0.5%, and 5.4% in Region 2. Although the T_s of 50 mm appreciably decreased, the T_s of 10 and 25 mm improved 2.1% and 3.2% in Region 1 within 24–48 h in the COMPARE1 experiment. And the T_s of 50 mm improved 4.6% in Region 1 within 24–48 h in the COMPARE2 experiment.

In conclusion, it is profitable to improve the heavy rainfall prediction by using the satellite radiance data to form the initial field. Particularly, the initial field using the AMSU-A microwave radiance data can signi-

Table 2. T_s score of rainfall from the three experiments in 2004.

		33°–50°N, 105°–125°E			20°–50°N, 95°–125°E		
Time	Degree	CONT	COMPARE1	COMPARE2	CONT	COMPARE1	COMPARE2
00–24 h	1 mm	57.75	57.22	54.57	63.20	58.72	56.65
	5 mm	33.36	31.49	29.04	42.25	37.57	34.28
	10 mm	21.35	21.79	21.50	29.07	29.63	26.22
	25 mm	11.02	11.37	10.81	19.07	19.43	19.16
	50 mm	3.11	3.52	3.6	9.38	9.62	9.73
24–48 h	1 mm	55.06	50.32	49.20	61.07	57.22	56.18
	5 mm	30.98	28.94	23.60	40.26	36.26	31.81
	10 mm	20.16	20.80	19.33	29.16	29.28	28.29
	25 mm	9.51	10.23	9.64	16.45	16.53	15.67
	50 mm	2.39	2.17	2.50	5.23	5.48	5.64

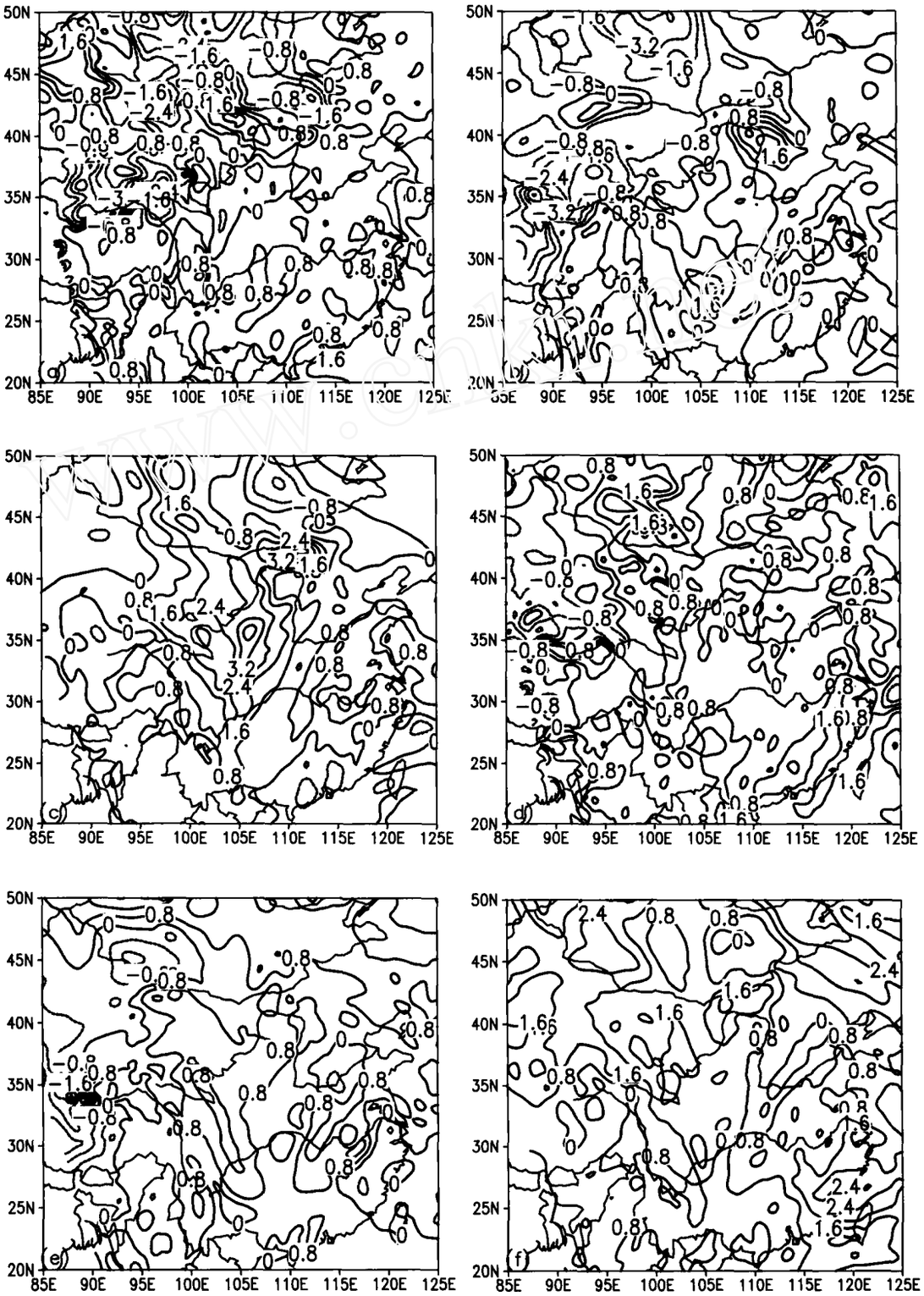

Fig. 7. The temperature difference of COMAPRE1 and CONT (a–c); COMPARE2 and CONT (d–f); (a), (d) on 850 hPa; (b)、(e) on 500 hPa; (c), (f) on 300 hPa at 0000 UTC 11 July 2004 (Units: °C).

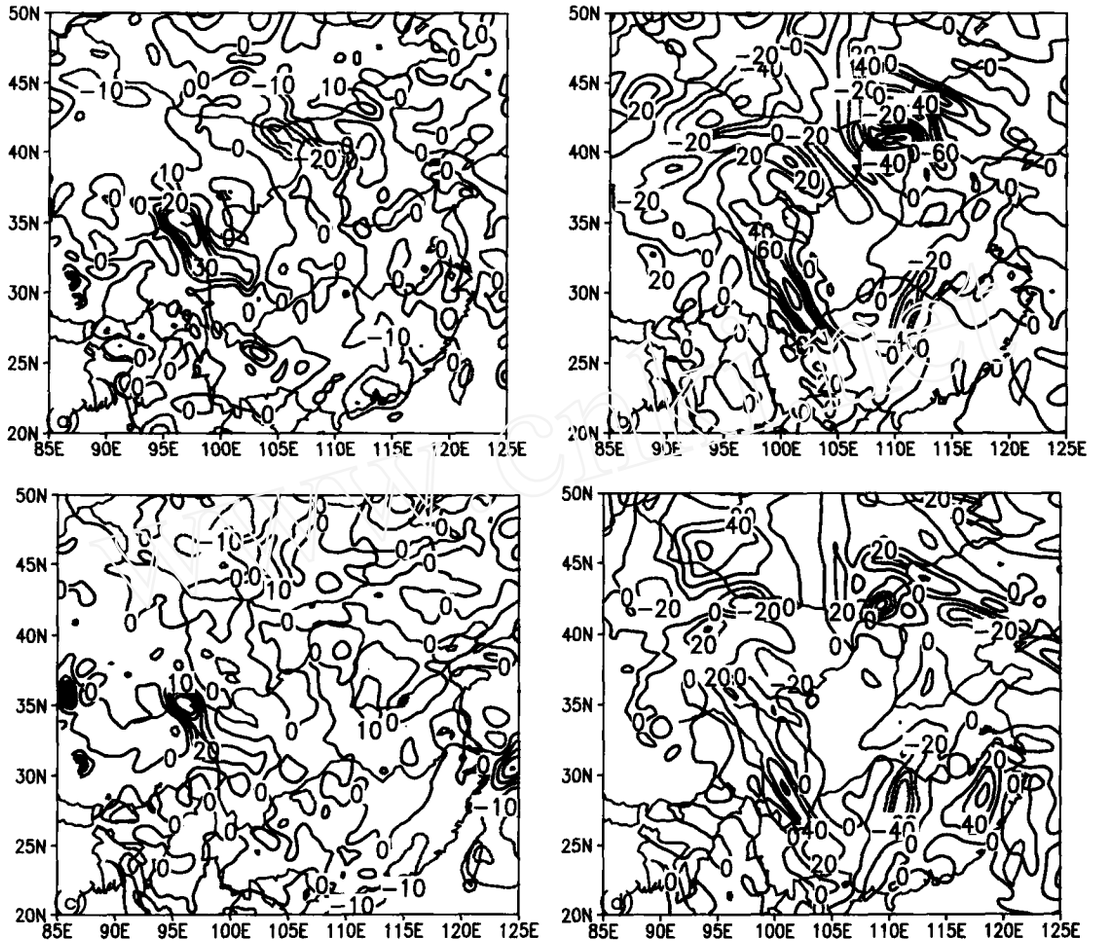

Fig. 8. The relative humidity difference of COMPARE1 and CONT (upper panel); COMPARE2 and CONT (lower panel); (a), (c) on 850 hPa; (b), (d) on 500 hPa at 0000 UTC 11 July 2004 (Units: %).

ficantly enhance the prediction of rainfall above 10 mm within 48 h. Although the initial field using the AMSU-B microwave radiance data could improve the prediction of rainfall above 50 mm within 24 h, it could not improve the rainfall prediction totally. By analysis, we found that using the AMSU-B microwave radiance data to modify the initial field can increase the local content of humidity, which makes a positive contribution to the occurrence of the convection. After the convection appears, the convergence will induce the concentration of the local humidity, which may increase the local heavy rainfall and reduce the rainfall area. In addition, the reason why using the ATOVS radiance data to form the initial field can improve the severe rainfall prediction but reduce the weak rainfall prediction will be further studied in the future.

4.4 *A heavy rainfall case*

From the above analyses, the statistical analysis of rainfall prediction is given. In the following, a severe rainfall case of 10–11 July 2004 is used to analyze the detailed effects of AMSU-A and AMSU-B data on the i nitial field and rainfall prediction. During 0000 UTC–2400 UTC 10 July 2004, the accumulated rainfall was more than 50 mm from 0800 UTC to 1200 UTC 10 July 2004 in the downtown area of Beijing, and a record-setting heavy rainfall of 125 mm occurred at Zizhuyuan Park. It is indicated that the local heavy rainfall in Beijing was caused by the mesoscale convective systems (MCSs). Three experiments, the same as in Table 1, are performed to determine the impact of ATOVS data on the simulation of this heavy rainfall.

The results of the three experiments are compared. The distribution and evolvement of the weather system are simulated successfully in the three experiments, including the intensity and position of the trough in the lower-middle troposphere and the intensity and track of the Low Level Jet (LLJ). However, in comparison

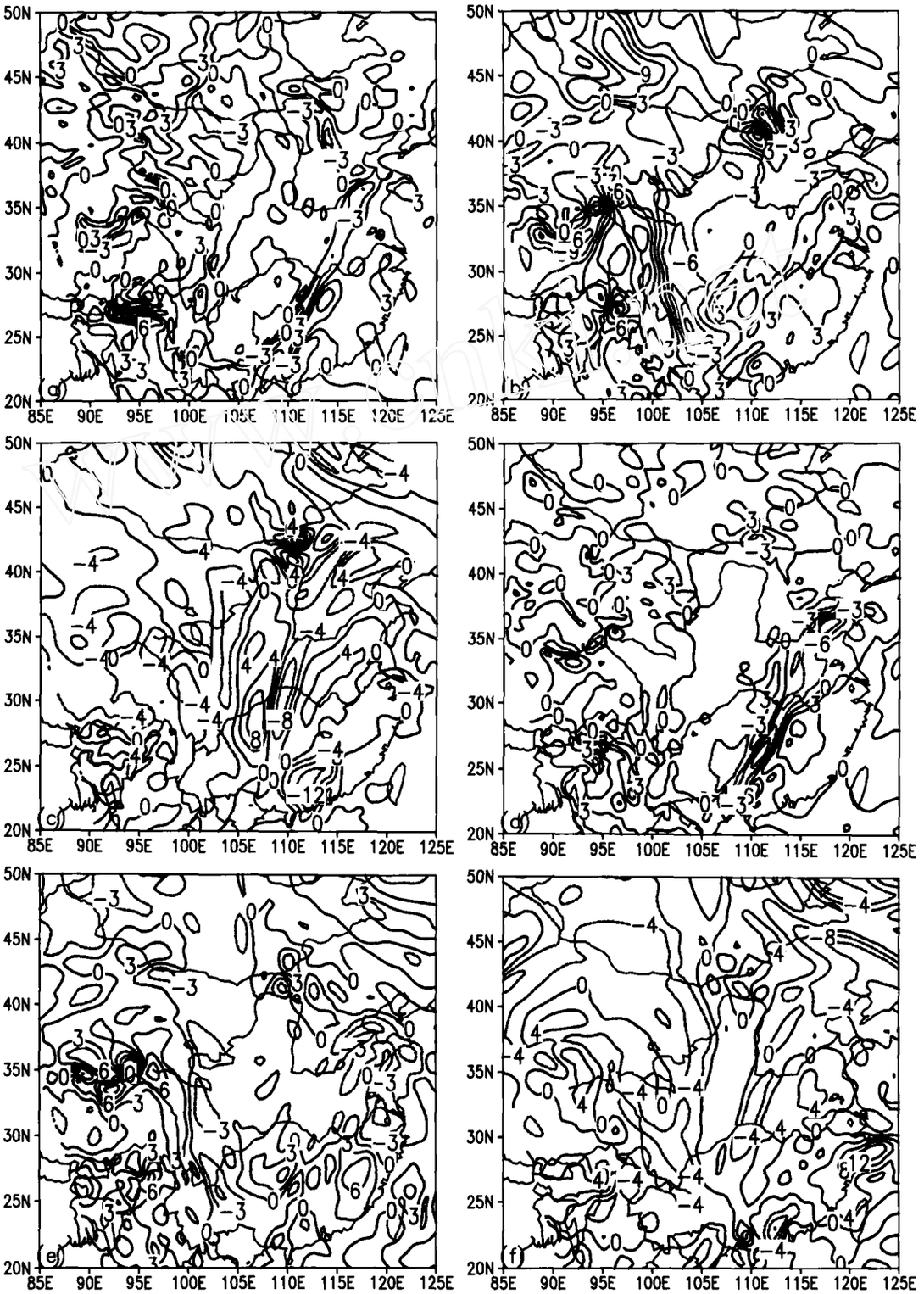

Fig. 9. The wind speed difference of COMAPRE1 and CONT (a–c); COMPARE2 and CONT (d–f); (a), (d) on 850 hPa; (b), (e) on 500 hPa; (c), (f) on 300 hPa at 0000 UTC 11 July 2004 (Units: m s^{-1}).

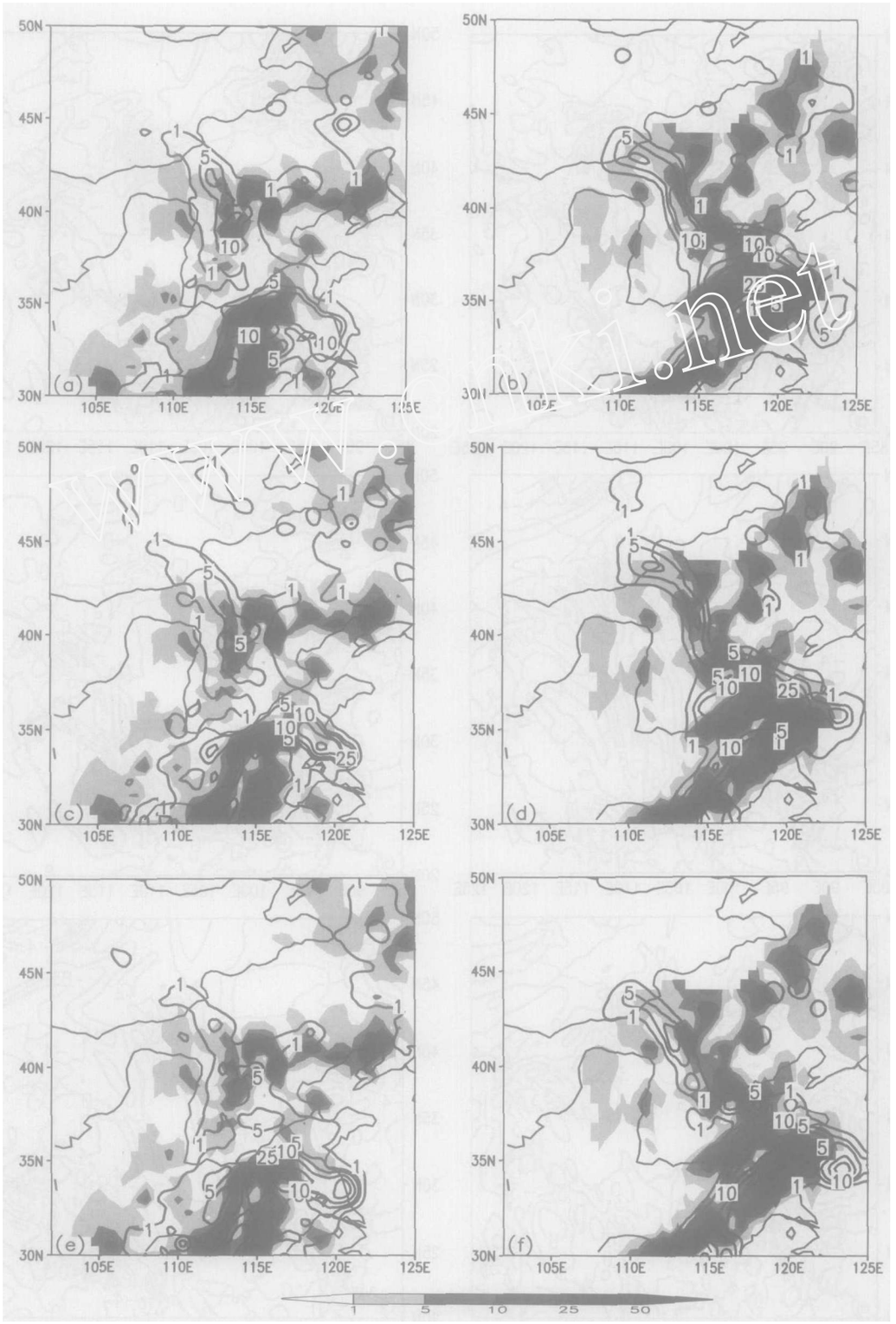

Fig. 10. The 6-h simulated precipitation from CONT (upper panel), COMPARE1 (middle panel), COMPARE2 (lower panel) and observational precipitation on (a), (c), (e) 0600 UTC–1200 UTC 10 July 2004, (b), (d), (f) 1800 UTC–2400 UTC 10 July 2004 (shaded: observations, contours: CONT, COMPARE1 and COMPARE2, Units: mm).

with the weak transportation of the moisture in the CONT and the COMPARE1 experiments, more moisture and strong transportation is obtained in the COMPARE2 experiment (Fig. 7 and Fig. 8). Generally, the temperature and moisture in the lower troposphere are relatively more important for rainfall prediction than that in the middle and upper troposphere. It is found that the AMSU-B data impact the temperature more significantly and the relative humidity more reasonably in the lower troposphere. It is also revealed in Figs. 7 and 8 that the influence of the ATOVS data is more extraordinary in North China. This may be caused by mesoscale characteristics that are not detected by conventional sounding observations. In addition, we compare the wind speed difference between the CONT, the COMPARE1 and the COMPARE2 experiments (Fig. 9). It is revealed that the simulated wind speed is not changed significantly over most of the model domain when the satellite radiance data are assimilated. The differences in the simulated wind speed mainly occur in the rain area and to the southeast of the rain area, and the wind speed in the troposphere of the COMPARE2 experiment is obviously strengthened near Beijing. Although the wind speed in the low and middle troposphere of the COMPARE1 experiment is also strengthened, the intensity is relatively weak. The slightly stronger simulated wind in COMPARE2 may explain the more severe simulated rainfall, which is propitious to the transportation of moisture. Therefore, the use of ATOVS data could improve the simulation of rainfall.

The rainfall predictions in the three experiments also have some remarkable differences. Figure 10 shows the 6-h simulated and observational precipitation during 0000 UTC–2400 UTC 10 July 2004. Although the rainfall in North China is not very close to the observations, the heavy rainfall occurring in the Huanghe River and Yangtze River basins is reproduced successfully. The severe heavy rainfall occurring from 0600 UTC to 1200 UTC 10 July 2004 is the most severe during this case, which was produced by mesoscale convective systems. Compared with the simulated rainfall of 0600 UTC–1200 UTC 10 July 2004 by the CONT and the COMPARE1 experiments, the intensity and position of the simulated rainfall in the COMPARE2 experiment are more similar to the observations in North China, especially in Beijing. Since the simulation schemes in the three experiments are the same, the slightly better simulated rainfall in COMPARE2 may be explained partially by there being more information on the mesoscale system in the initial condition. All the simulated results imply that although some deficiencies exist in the simulation of the mesoscale convective system and the heavy rainfall occurring in North China, the direct assimilation of ATOVS data makes a certain improvement in the rainfall prediction.

5. Summary and Conclusions

To understand the impact of satellite radiance data on the initial fields and rainfall prediction, the 3D-VAR assimilation technique is used to directly assimilate the AMSU-A and AMSU-B microwave radiance data. Subsequently, the assimilation results from the GRAPES_3D-VAR system are utilized as the initial field to predict the rainfall in summer 2004. According to the analyses from the experiments, the following conclusions are obtained:

(1) The GRAPES_3D-VAR system developed by CMA was proved to be effective for directly assimilating satellite radiance data as well as conventional observations.

(2) The AMSU-A and AMSU-B radiance data have a certain impact on the geopotential height, temperature, relative humidity and flow field. Furthermore, the impacts on the background field are mostly similar in different months in the summer.

(3) The AMSU-A radiance data can significantly enhance the prediction of rainfall above 10 mm within 48 h, and the AMSU-B microwave radiance data can improve the prediction of rainfall above 50 mm within 24 h.

(4) With the rapid development of atmospheric theory and the remote sensing sounding techniques, the era of relying on the unconventional satellite observations is coming. The results of the experiments in our study and the previous studies show that the ATOVS microwave radiance data and its assimilation technique is an effective way to solve the problem of the lack of conventional observation data over some prediction domain, and this has great potential and brilliant prospects in heavy rainfall prediction.

In addition, this study is preliminary at present, and the analysis cannot describe the detailed impact of the satellite radiance data. Hence, further analysis needs to be done.

Acknowledgments. The support of the National Key Basic Research and Development Project of China (Grant No. 2004CB418300) and the Chinese Academy of Sciences Project (Grant No. KACX1–02) is gratefully acknowledged. Acknowledgments are also given to Dr. Zhu Guofu and Dong Peiming of the Chinese Academy of Meteorological Sciences for aiding this research.

REFERENCES

Andersson, E., J. Pailleux, J.-N. Thepaut, J. R. Eyre, A. P. McNally, G. A. Kelly, and P. Courtier, 1994: Use of cloud-cleared radiance in three/four-dimensional variational data assimilation. *Quart. J. Roy. Meteor. Soc.*, **120**, 627–653.

Courtier, P., 1997: Variational methods. *J. Meteor. Soc. Japan*, **75**(1B), 211–218.

Courtier, P., and Coauthors, 1996: The ECMWF implementation of three-dimensional variational assimilation (3D-Var). I: Formulation. *Quart. J. Roy. Meteor. Soc.*, **124**, 1783–1807.

Derber, J. C., and W. S. Wu, 1998: The use of TOVS cloud-cleared radiances in the NCEP SSI analysis system. *Mon. Wea. Rev.*, **126**, 2287–2299.

Dudhia, J., 1993: A nonhydrostatic version of the Penn State-NCAR mesoscale model: Validation tests and simulation of an Atlantic cyclone and cold front. *Mon. Wea. Rev.*, **121**, 1493–1513.

Eyre, J. R., G. A. Kelly, A. P. McNally, E. Andersson, and A. Persson, 1993: Assimilation of TOVS radiance information through one-dimensional variational analysis. *Quart. J. Roy. Meteor. Soc.*, **119**, 1427–1463.

Ge Wenzhong, Dang Renqing, Jiang Dunchun, Xu Hui, and Takao Tekeda, 1998: Application of radar and satellite data for numerical simulation of heavy rainfall. *International Symposium on Mesoscale Water Cycle and Heavy Rainfall in East Asia*, Nagoya, Japan, 2–4 Feb. 123–126.

Ge Wenzhong, Dang Renqing, Xu Zhifang, and Takao Takeda, 2000: The impact of assimilations of radar and satellite data on numerical simulation of heavy rainfall. *International GAME/HUBEX Workshop*, Hokkaido University, Sapporo, 93–96.

Grell, G. A, J. Dudhia, and D. R. Stauffer, 1994: A description of the fifth-generation Penn State/NCAR mesoscale model (MM5). NCAR Technical Note, NCAR/TN-398+STR, 138pp.

Jiang Dunchun, Dang Renqing, and Chen Lianshou, 1994: The use of satellite data in the numerical prediction model for the study of the heavy rainfall caused by typhoon. *Journal of Tropical Meteorology*, **10**(4), 318–324. (in Chinese)

Lorenc, A. C., 1997: Development of an operational variational assimilation scheme. *J. Meteor. Soc. Japan*, **75**(1B), 339–346.

Menzel, W. P., and A. Chedin, 1990: Summary of the Fifth International TOVS Study Conference. *Bull. Amer. Meteor. Soc.*, **71**, 691–693.

McNally, A. P., E. Andersson, and G. Kelly, 1999: The use of raw TOVS/ATOVS radiances in the ECMWF 4D-Var assimilation system. *Technical Proc. of the 10th International ATOVS Study Conference*, Boulder, Colorado, USA, 27 January–2 February, 377–384.

Ninomiya, K., and K. Kurihara, 1987: Forecast experiment of a long-lived mesoscale convective system in Baiu frontal zone. *J. Meteor. Soc. Japan*, **65**, 885–899.

Parrish, D. F., and J. C. Derber, 1992: The National Meteorological Center's Spectral Statistical Interpolation analysis system. *Mon. Wea. Rev.*, **120**, 1747–1763.

Pan Ning, Dong Chaohua, and Zhang Wenjian, 2003: The experiments on direct assimilating ATOVS radiance. *Acta Meteorologica Sinica*, **61**(2), 226–236. (in Chinese)

Qi Linlin, 2003: Chapter 6, The application of ATOVS radiance data on the simulation of sudden severe heavy rainfall in Shanghai on August 2001. Ph. D. dissertation, Institute of Atmospheric Physics, Chinese Academy of Sciences, 89–102. (in Chinese)

Rabier, F., H. Jarvinen, E. Klinker, J. F. Mahfouf, and A. Simmons, 2000: The ECMWF implementation of four-dimensional variational assimilation I: Experimental results with simplified physics. *Quart. J. Roy. Meteor. Soc.*, **126**, 1143–1170.

Smith, W. L., G. S. Wade, and H. M. Woolf, 1985: Combined atmospheric sounder/cloud imagery—A new forecasting tool. *Bull. Amer. Meteor. Soc.*, **66**, 138–141.

Turpeinen, O. M., L. Garand, R. Benoit, and M. Roch, 1990: Diabatic initialization of the Canadian Regional Finite Element (RFE) model using satellite data. Part I: Methodology and application to a winter storm. *Mon. Wea. Rev.*, **118**, 1381–1407.

Wang Zihou, Wang Zonghao, and Zhang Fengying, 1995: A study of application of HIRS/2 brightness temperature to NWP without retrieval. *Quarterly Journal of Applied Meteorology*, **6**(3), 273–280. (in Chinese)

Weng, F., and N. Grody, 2000: Retrieval of ice cloud parameters using a microwave imaging radiometer. *J. Atmos. Sci.*, **57**, 1069–1081.

Weng Yonghui, and Xu Xiangde, 1999: Numerical simulation over the Tibetan Plateau by using variational technique revised TOVS data. *Chinese Journal of Atmospheric Sciences*, **23**(6), 703–712. (in Chinese)

Wolcott, S. W., and T. T. Warner, 1981: A moisture analysis procedure utilizing surface and satellite data. *Mon. Wea. Rev.*, **109**(9), 1989–1998.

William, S., 1991: Atmospheric soundings from satellites-False expectation or the key to improved weather prediction. *Quart. J. Meteor. Soc.*, **117**, 267–297.

Xue Jishan, and Coauthors, 2001: Scientific design scheme of the GRAPES 3D-Var system. Tech. Rep, Numerical Weather Prediction Center, Chinese Academy of Meteorological Sciences. 140pp.

Zhang Fengying, 2002: Characteristics of the new atmospheric sounder ATOVS and its data processing method. Tech. Rep, National Satellite Meteorological Center, 56pp. (in Chinese)

Zhang Hua, Xue Jishan, Zhu Guofu, Zhuang Shiyu, Wu Xuebao, and Zhang Fengying, 2004: Application of direct assimilation of ATOVS microwave radiances to typhoon track prediction. *Adv. Atmos. Sci.*, **21**(2), 283–290.

Zhu Min, Yu Fan, Zheng Weizhong, Yu Zhihao, Lu Hancheng, and Liu Changsheng, 2000: The study of preliminary application of satellite-derived relative humidity in rainstorm forecast. *Acta Meteorological Sinca*, **58**(4), 470–478. (in Chinese)